Monthly Notices
of the
ROYAL ASTRONOMICAL SOCIETY

MNRAS **442,** 1319–1325 (2014) doi:10.1093/mnras/stu869

Do cement nanoparticles exist in space?

G. Bilalbegović,[1]★ A. Maksimović[2] and V. Mohaček-Grošev[2]

[1]*Department of Physics, Faculty of Science, University of Zagreb, Bijenička 32, 10000 Zagreb, Croatia*
[2]*Rudjer Bošković Institute, Bijenička 54, 10000 Zagreb, Croatia*

Accepted 2014 April 29. Received 2014 April 29; in original form 2014 March 5

ABSTRACT

Calcium silicate hydrate is used to model the properties of cement on Earth. We study cementitious nanoparticles and propose these structures as components of cosmic dust grains. Quantum density functional theory methods are applied for the calculation of infrared spectra of $Ca_4Si_4O_{14}H_4$, $Ca_6Si_3O_{13}H_2$ and $Ca_{12}Si_6O_{26}H_4$ clusters. We find bands distributed over the near-, mid- and far-infrared regions. A specific calcium silicate hydrate spectral feature at 14 μm, together with bands at 10 and 18 μm, which exist for other silicates as well, could be used for the detection of cosmic cement. We compare the calculated bands with the 14-μm features in the spectra of HD 45677, HD 44179 and IRC+10420, which were observed by the *Infrared Space Observatory* and classified as remaining. A high abundance of oxygen atoms in cementitious nanoparticles could partially explain the observed depletion of this element from the interstellar medium on to dust grains.

Key words: astrochemistry – methods: numerical – ISM: abundances – infrared: general.

1 INTRODUCTION

Dust is produced in supernova explosions and the outflows of stars (Draine 2011; Tielens 2013). It is very important in the evolution of stars and galaxies. Dust grains act as a substrate for the formation of H_2 and many other astrophysical molecules, including prebiotic ones. It is accepted today that cosmic dust consists of silicates and carbonaceous materials with impurities from several chemical elements. Using infrared spectroscopy, both silicates and carbon-based grains have been observed in various environments: close to Earth and exoplanets, in the interstellar medium, in comets, around stars and in active galactic nuclei. The light from cosmic objects heats dust grains, which is followed by dust emission in the infrared spectral region. Absorption features in the infrared produced by dust are also observed. The size of grains is from the length of one molecule up to several hundred micrometres. It is known that 10 per cent of grains are ultra-small, with a size around 1.5 nm or less (Li & Draine 2001).

Cosmic dust mainly forms from the most abundant elements, such as silicon, carbon, oxygen, iron and magnesium. Calcium is one of the chemical elements that are produced in supernova explosions. It belongs to the group of 20 most abundant chemical elements in the Universe. The Ca II absorption line was one of the first lines discovered in interstellar space (Hartmann 1904). It has been proposed that compounds containing calcium exist in space. For example, spectra of Ca-poor and Ca-rich pyroxenes have been measured in mid- and far-infrared wavelengths in laboratories on Earth (Koike et al. 2001). It has been suggested that the amorphous diopside, $CaMgSi_2O_6$, contributes to the far-infrared spectrum of the planetary nebula NGC 6302. Calcium has been measured in meteorites and rocks of Mars, where it is a component in calcium–aluminum-rich inclusions and chondrules (Simon, DePaolo & Moynier 2009).

Calcium compounds are the main constituents of cement, which is one of the most used materials on Earth (Allen, Thomas & Jennings 2007; Pellenq et al. 2009; Skinner et al. 2010; Masoero et al. 2012). Cement paste is formed when cement powder, consisting mainly of alite (Ca_3SiO_5) and belite (Ca_2SiO_4), is mixed with water. Calcium silicate hydrate has a granular complex structure. Its chemical composition is variable, being characterized by $CaO:SiO_2$ ratios in the range 0.7–2.3 (Manzano, Ayuela & Dolado 2007). It has been found that temperatures above 350 K are necessary for the reaction between H_2O gas molecules and silicates in the outflows of stars (Grossman & Larimer 1974). However, silicate cosmic dust grains are often covered with water ice mantles. H_2O from mantles could react with silicates and calcium atoms and form a cosmic cement paste. We expect that cementitious materials could be produced as a dust component around oxygen-rich stars where silicates are dominant. The presence in space of various minerals in the form of hydrous silicates (for example talc, $Mg_3[Si_4O_{10}|(OH)_2]$, and montmorillonite, $(Mg,Al)_2[Si_4O_{10}|(OH)_2](Na,K,Ca)_x \cdot nH_2O$) has been under discussion for some time (Whittet et al. 1997; Hofmeister & Bowey 2006; Mutschke et al. 2008).

Infrared spectroscopy is used in the field of solid-state astrophysics (Jager et al. 2011) and astronomical observations are compared with spectra measured in laboratories. For example, spectra between 2.4 and 195 μm for 17 oxygen-rich circumstellar dust shells were observed using the Short and Long Wavelength Spectrographs

★ E-mail: goranka.bilalbegovic@gmail.com

on the *Infrared Space Observatory* (*ISO*) and compared with laboratory measurements (Molster et al. 2002a; Molster, Waters & Tielens 2002b). Although many bands were fitted with measured spectra of Mg-rich olivines and pyroxenes, 20 per cent of the spectral features were not identified. The *Spitzer* and *Herschel* missions collected many infrared spectra of dust grains (Watson et al. 2009; Ciesla et al. 2014). In laboratory measurements, in order to model various cosmic conditions, spectra of materials are studied from very low temperatures up to 1000 K. However, the interpretation of measured infrared spectra of complex materials can often be involved. Infrared spectroscopy of nanoparticles is even more demanding in comparison with measurements of the bulk material. Computational infrared studies of dust materials provide a connection between the microscopic structure and spectral properties. This is very important in astrophysics. For example, because of astronomical emissions at 3.3, 6.2, 7.7, 8.6, 11.2 and 12.7 μm, infrared spectra of polycyclic aromatic hydrocarbons (PAHs) have been calculated and assembled in a spectroscopic data base (Bauschlicher et al. 2010; Boersma et al. 2014). Recently, spectra of PAH clusters have been calculated (Ricca, Bauschlicher & Allamandola 2013). Infrared spectra of a dust-grain model in the form of the bare nanopyroxene cluster $Mg_4Si_4O_{12}$, as well as its hydrogenated and oxygenated forms, have also been calculated by quantum computational methods (Goumans & Bromley 2011).

Various crystalline and amorphous forms of silicates with different sizes, shapes and chemical compositions could form under diverse conditions in space (Henning 2010). We have selected three clusters that consist of Ca, Si, O and H atoms. Using these nanoparticles, we model the crystalline and amorphous states of possible ultra-small cosmic dust grains with the structure of cement paste. Density functional theory computational methods (Martin 2004) are used to study the structural properties of these nanoparticles, calculate vibrational modes and explore important features in their infrared spectra.

2 COMPUTATIONAL METHODS

The accepted model of cosmic silicates is an arrangement of small silicate particles of different sizes (Henning 2010). We study three nanoparticles that exhibit the typical bonding and small-scale structure of the cement paste. These three models of ultra-small cosmic particles are selected to represent crystalline and amorphous cosmic silicates, both found in cosmic dust. One cluster, $Ca_4Si_4O_{14}H_4$ (labelled as C1 in the following text), is chosen to model a crystalline state of any possible cosmic cement. This cluster has been modelled on the previous Hartree–Fock calculation on the formation of cementitious nanoparticles (Manzano et al. 2007). The structure of C_1 has been proposed by Manzano et al. as a common precursor of both tobermorite and jennite bulk crystal structures of calcium silicate hydrate. The same C_1 structure, but in a narrower spectral region, has been studied using the semi-empirical Modified Neglect of Diatomic Overlap and density functional theory methods (Bhat & Debnath 2011). We also study two amorphous nanoparticles, $Ca_6Si_3O_{13}H_2$ (C2 in the following text) and $Ca_{12}Si_6O_{26}H_4$ (labelled as C3). They have been cut from the bulk of the calcium silicate hydrate presented in the Materials Project (Jain et al. 2013). The clusters are characterized by $CaO{:}SiO_2$ ratios of 1 (in C1) and 2 (in C2 and C3). One (in C2) and two (in C1 and C3) units of water (2H and O) are present.

We have used the real-space Grid based Projector Augmented Wave method (GPAW) density functional program package (Enkovaara et al. 2010) and its Atomistic Simulation Environment (ASE) user interface (Bahn & Jacobsen 2002). The Perdew-Burke-Ernzerhof (PBE) generalized gradient approximation (GGA) exchange-correlation functional (Perdew, Burke & Ernzerhof 1996) and the Projector-Augmented Wave (PAW) pseudopotentials (Mortensen, Hansen & Jacobsen 2005) are applied. The C1 cluster is optimized globally. We use the Monte Carlo basin-hopping algorithm (Wales & Doye 1997; Wales & Scheraga 1999) as implemented in ASE. All interactions in this optimization are treated within GPAW, at the same density functional theory level (i.e. using the GGA functional and the PAW pseudopotentials). It is known that the Monte Carlo basin-hopping algorithm method is very successful in finding minima of clusters (Bilalbegovic 2003; Goumans & Bromley 2011; Jiang & Walter 2011). Infrared spectra are calculated using the finite-difference approximation, for both the dynamical matrix and the gradient of the dipole momentum of the system (Porezag & Pederson 1996; Frederiksen et al. 2007). In this method, the infrared intensity I_i of mode i is calculated from

$$I_i = \frac{\mathcal{N}\pi}{3c}\left|\frac{\mathrm{d}\boldsymbol{\mu}}{\mathrm{d}Q_i}\right|^2, \quad (1)$$

where $\mathcal{N}$ is the particle density, c is the velocity of light, μ is the electric dipole momentum and Q_i is the coordinate of the normal mode. The GPAW code and the PBE GGA functional have recently been employed to calculate the infrared spectrum of thiol-stabilized gold nanoclusters (Hulkko et al. 2011). These results have been compared with measurements and very good agreement is found. Our results for the crystalline C1 cluster agree with the calculations of Bhat and Debnath, which have been carried out at local density approximation (LDA) and GGA Becke-Lee-Yang-Parr (BLYP) levels (Bhat & Debnath 2011). Two bands in the spectra of amorphous clusters C2 and C3 agree with laboratory measurements on calcium silicate smoke samples in the mid-infrared region (Kimura & Nuth 2005).

3 RESULTS AND DISCUSSION

Optimized structures for the cementitious clusters we have studied are shown in Fig. 1. We have found that clusters C2 and C3 are less stable than the crystalline precursor C1. A small displacement of atoms from the structures of C2 and C3, corresponding to their local minima, quickly leads to bigger forces between atoms. Potential energies are -6.771 eV atom^{-1} (C1), -6.668 eV atom^{-1} (C3) and -6.476 eV atom^{-1} (C2). When compared with C2, the cluster C3 has all numbers of atoms doubled. However, C2 is less stable than C3. Clusters C2 and C3 represent amorphous nanoparticles that could form under various conditions of temperature, pressure, radiation and shock waves in space. In contrast, the structure of C1 is very stable, which confirms the idea of Manzano et al. (Manzano et al. 2007) that this cluster is a building block of cement on Earth. Clusters C2 and C3 are examples of the many possible amorphous silicate nanoparticles in space. We have calculated that, in addition to the specific cement band at 14 μm, amorphous clusters C2 and C3 exhibit the typical bands of amorphous cosmic silicates at 10 and 18 μm. This shows that our models of amorphous cement nanoparticles are reliable. Both amorphous and crystalline silicates have been observed in cosmic dust (van Boekel et al. 2005). Amorphous silicates are typical for the interstellar medium, whereas in circumstellar discs both crystalline and amorphous silicates exist. Crystalline silicates are also found in comets and dust particles in the Solar system. Infrared spectra are used for the analysis of these various forms of silicate cosmic dust (Kessler-Silacci et al. 2006; Henning 2010; Draine 2011).

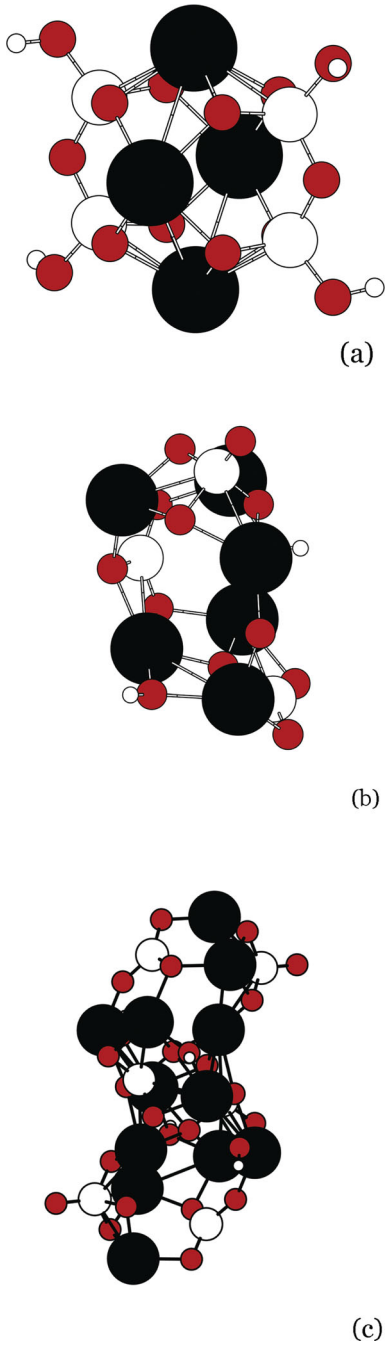

Figure 1. The geometry of cementitious clusters: (a) C1: $Ca_4Si_4O_{14}H_4$, (b) C2: $Ca_6Si_3O_{13}H_2$ and (c) C3: $Ca_{12}Si_6O_{26}H_4$. Small white balls represent hydrogen atoms, grey (red in the colour figure) are for oxygen, large white for silicon and black for calcium atoms.

In the majority of bulk silicates, the Si atom is positioned in tetrahedra of oxygen atoms. In the mineralogy of silicates, several complex structures are known, for example two tetrahedra sharing one oxygen atom (as in gehlenite $Ca_2Al_2SiO_7$) or tetrahedra that form rings (as in the beryl $Be_3Al_2Si_6O_{18}$). Several other arrangements of chains and rings exist in various silicates. Hydrous silicates belong to the group of phyllosilicates, where layers of silicates and OH layers appear. Higher coordination numbers in silicates are also known. For example, an octahedral configuration of Si occurs under high pressures or in the mineral thaumasite,

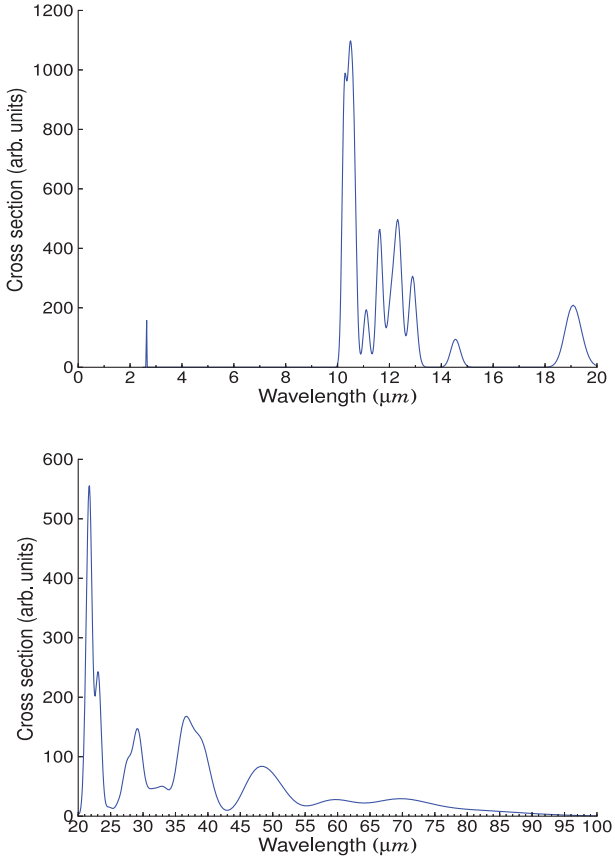

Figure 2. Infrared spectrum of the C1 cluster.

$Ca_3Si(OH)_6(CO_3)(SO_4)\cdot 12H_2O$. Thaumasite sometimes forms in cements when their main components are exposed to sulphates (Nobst & Stark 2003). We have found that in the C1 cluster all silicon atoms are tetrahedrally coordinated. In C2, two Si atoms are surrounded by three oxygens and one by four O atoms. Four Si atoms are tetrahedrally coordinated and two silicon atoms have three nearest oxygen neighbours in the C3 cluster.

Infrared spectra (calculated for nanostructures presented in Fig. 1) are shown in Figs 2–4. Theoretical results for infrared spectra consist only of vertical lines. In contrast, in measured astronomical infrared spectra these lines are broad and reflect the conditions of the observed objects (Bauschlicher et al. 2010). It is common practice to broaden theoretical lines. We use Lorentzian band profiles with a full width at half-maximum (FWHM) of 20 cm^{-1}. Bands with higher intensities, calculated using equation (1), are shown in Table 1.

Lines with a small intensity exist in the near-infrared region at 2.62, 2.64 and 2.65 μm for C1 (Fig. 2), 2.63 and 2.69 μm for C2 (Fig. 3) and 2.64, 2.66 and 2.67 μm for C3 (Fig. 4). For C1, Bhat and Debnath calculated 2.63 (in LDA) and 2.67 μm (in GGA BLYP) (Bhat & Debnath 2011). A spectral region at ∼(2–4) μm is known as the water ice band (Gibb et al. 2004). The interval (2.6–2.8) μm corresponds to vibrations of O–H in hydrated silicates. The water ice band has been studied in the astrophysical context because of various hydrosilicate minerals (Whittet et al. 1997; Hofmeister & Bowey 2006; Mutschke et al. 2008) or H_2O trapped and adsorbed in the SiO condensate (Wada, Sakata & Tokunaga 1991).

Bands in the near-infrared and the start of the mid-infrared region have been found in laboratory measurements of CaO and $Ca(OH)_2$ grains and the measured line at 6.8 μm has been proposed to explain

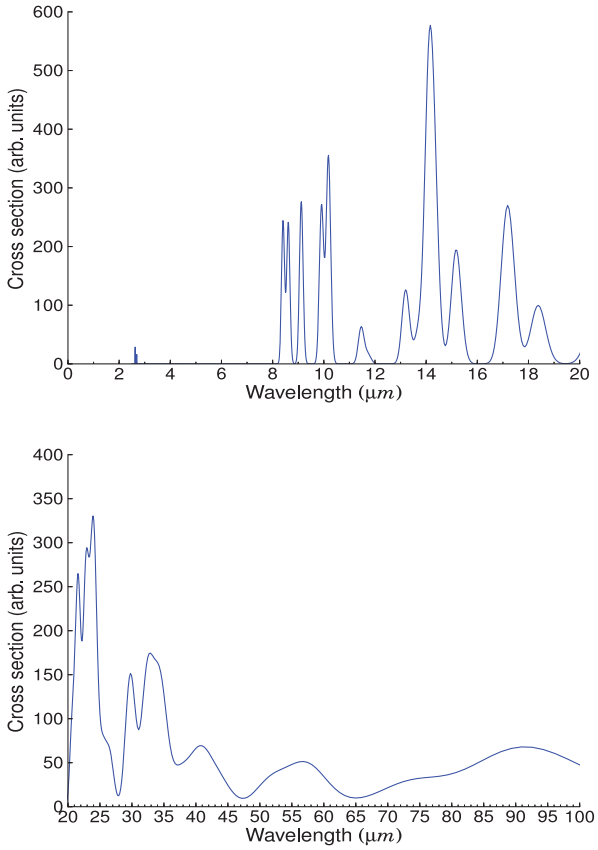

Figure 3. Infrared spectrum of the C2 cluster.

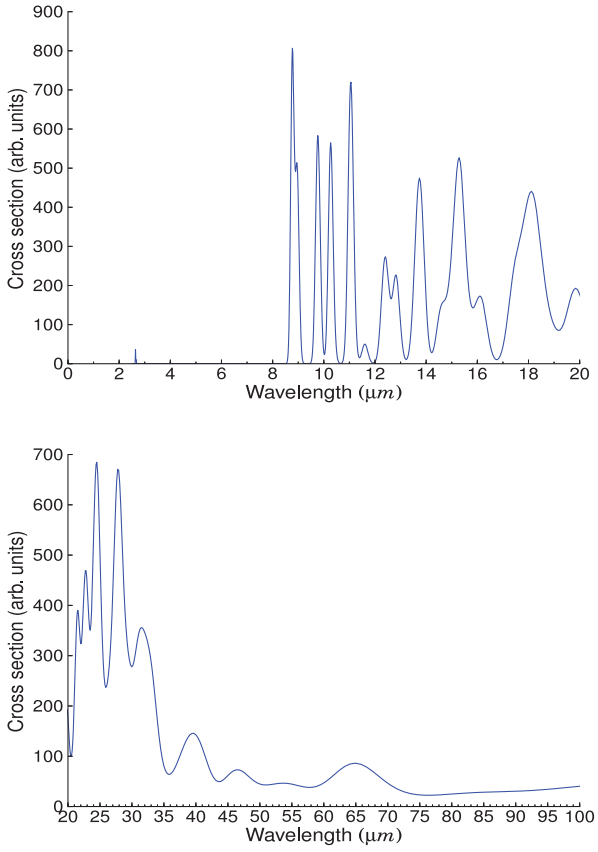

Figure 4. Infrared spectrum of the C3 cluster.

this feature in the spectra of young stellar objects (Kimura & Nuth 2005). Typical features of amorphous silicates in the mid-infrared are broad bands at 10 and 18 μm, which correspond to the Si–O stretching and O–Si–O bending modes. Silicate bands in the far-infrared also exist and are attributed to metal–oxygen modes.

In the mid-infrared region of the C1 cluster (Fig. 2 and Table 1) we found five close bands at 10 μm: 10.26, 10.29, 10.40, 10.47 and 10.63 μm. In addition, we have calculated several bands of smaller intensity between 11 and 13 μm, as well as at 14.44, 14.55 and 19.08 μm. Several bands appear above 20 μm, the strongest ones being at 21.73 and 23.11 μm. The far-infrared spectrum is broad and with small intensity. The main bands in this region are at 36.44 and 38.76 μm. Bhat and Debnath, for the mid-infrared region of C1, also found no lines below 10 μm in their GGA BLYP approximation, but such lines appear in LDA (Bhat & Debnath 2011). Our other calculated lines in the mid-infrared are in good agreement with their results. They did not calculate bands above 22 μm.

In the mid-infrared spectral region of the C2 cluster (Fig. 3 and Table 1), bands appear also slightly below 10 μm: 8.41, 8.61, 9.12 and 9.91 μm. There are strong bands at 10.18, 14.32 and 17.18 μm. Several other bands of smaller intensity exist between 10 and 20 μm. For the C2 cluster, many bands appear above 20 μm. The strongest bands in this region are at 22.90, 24.03, 29.9 and 34.47 μm. In the mid-infrared spectral region of the C3 cluster (Fig. 4 and Table 1), stronger bands are close to 8, 9, 10, 11, 12, 13, 14, 15, 16, 17, 18, 19, 21, 22, 24, 27, 29 and 30 μm. Weaker bands exist above 30 μm. A rather strong band (with an intensity of 71.98 km mol^{-1}) is calculated at 64.93 μm. The calcium silicate compound diopside $CaMgSi_2O_6$, proposed as a contributor to the far-infrared spectrum of the planetary nebula NGC 6302, shows the band at 65 μm (Koike et al. 2001).

Infrared spectroscopy is utilized for a characterization of bulk cementitious systems, but results depend on the variable chemical and structural composition of these materials (Yu et al. 1999; Garbev et al. 2007). Belite (Ca_2SiO_4) is one of the most important components of cement paste. In β-Ca_2SiO_4, a symmetrical stretching vibration of SiO_4 tetrahedra is assigned to bands measured at 11.57 and 11.74 μm (Bensted 1976). In alite (Ca_3SiO_5), which is also a major component of cement, weak bands exist at 6.42, 6.79 and 7.04 μm and strong ones at 10.64, 11.01, 11.32, 12.30, 18.98 and 22.08 μm (Delgado, Paroli & Beaudoin 1996). In hydrated cement paste, where the ratio CaO/SiO_2 is 1.5, stronger bands appear at 30.03 (Ca–O lattice vibrations), 22.47 (O–Si–O bending vibrations in SiO_4), 14.88 (assigned to the bending of two connected SiO_4 tetrahedra), 11.25 and 9.78 μm (both assigned to the symmetric stretching of SiO_4 tetrahedra) (Garbev et al. 2007). Bands in the near-infrared region (at 6.1, 2.89, 2.81 and 2.76 μm) that correspond to OH stretching vibrations in water and $Ca(OH)_2$ also exist in the spectra of hydrated cement paste. The most intense peak of cement is at 14.88 μm. This is the dominant and specific band for all hydrated cement paste compositions, i.e. for ratios of CaO/SiO_2 between 0.2 and 1.5 (Garbev et al. 2007).

Spectral features at 9.2 and 21.7 μm have been measured for calcium silicate smoke grains prepared in the laboratory by vapour phase condensation in the study of CaO and $Ca(OH)_2$ cosmic dust (Kimura & Nuth 2005). Close bands exist for C2 (9.12 and 21.64 μm) and C3 (8.99 and 21.50 μm). A specific 14-μm band of bulk cement paste is present in the spectra of clusters. We have found that bands at 14.44 and 14.55 μm (Fig. 2) exist for the most stable nanoparticle C1. This should be compared with the strong bands for C2 at 14.10 μm (Fig. 3) and for C3 at 14.58 μm (Fig. 4). There is a strong band for C3 at 11.05 μm, whereas in this region

Table 1. Infrared bands for the C1, C2 and C3 clusters. Only bands with intensities above 70 km mol^{-1} are shown for C1, above 60 km mol^{-1} for C2 and above 130 km mol^{-1} for C3.

C1		C2		C3	
Band (μm)	Intensity (km mol^{-1})	Band (μm)	Intensity (km mol^{-1})	Band (μm)	Intensity (km mol^{-1})
2.64	70.19	8.41	243.78	8.77	493.45
10.26	820.40	8.61	240.98	8.92	264.52
10.40	93.81	9.12	277.37	8.99	282.56
10.47	786.97	9.91	269.79	9.74	382.20
10.63	671.12	10.18	354.15	9.81	262.97
11.11	183.01	11.46	62.57	10.27	558.72
11.61	136.73	13.20	126.10	11.05	721.71
11.62	249.77	14.10	434.48	12.34	153.84
12.04	178.55	14.32	257.23	12.46	152.52
12.23	179.10	15.17	195.06	12.82	221.98
12.35	127.78	17.18	252.09	13.63	183.52
12.38	240.04	18.38	99.73	13.79	343.60
12.89	291.28	20.60	64.24	14.58	130.18
14.55	89.18	21.53	106.24	15.23	282.64
19.08	208.14	21.64	140.84	15.38	252.60
21.22	99.59	22.90	225.48	16.16	152.34
21.73	456.31	24.03	266.20	17.55	159.32
23.11	194.16	29.90	111.93	18.02	252.91
27.51	75.10	32.52	82.82	18.29	189.30
29.22	135.31	34.47	128.14	19.84	185.78
36.44	126.24			21.47	144.24
				21.50	162.64
				22.86	289.28
				24.18	141.95
				24.30	143.60
				24.59	324.46
				27.84	496.63
				29.42	158.36
				30.95	164.26

a weak band at 11.46 μm exists for C2 and at 11.62 μm for C1. Bands at 18 μm are also typical for amorphous cosmic silicates. For amorphous clusters, bands appear at 18.38 μm (C2) and at 18.02, 18.29, 18.58 and 18.99 μm (C3). Bands at 18 μm do not exist for the crystalline precursor C1. While bands around (10–11) and 18 μm appear in spectra of other silicates, features at 14 μm can be used to characterize cement nanoparticles.

Bands at 14 μm have been observed by the *Infrared Space Observatory* in the spectra of objects from a sample of 17 oxygen-rich circumstellar dust shells (Molster et al. 2002a,b). Weak features at 13.8 and 14.2 μm have been measured and classified as remaining bands or '(partly) instrumental'. For example, bands at 13.5, 13.8 and 14.3 μm in the spectrum of HD 45677 have been clearly detected. Other examples of band observations around 14 μm in the same sample are from the objects HD 44179, Roberts 22 and IRC+10420. However, silicate bands at 10 and 11 μm have not been observed for Roberts 22 (Molster et al. 2002a). A silicate band at 18 μm exists for this object. In contrast, silicate bands in both regions have been found in the spectra of HD 45677, HD 44179 and IRC+10420. We expect that exact positions of cement bands could vary with the composition and size of nanoparticles. To facilitate a comparison, in Table 2 the typical silicate and cement bands for the nanoparticles we studied are presented, together with the corresponding silicate and unidentified bands in the spectra of HD 45677, HD 44179 and IRC+10420 (Molster et al. 2002a). In Table 3, bands above 19 μm are compared. Bands for cement nanoparticles of various compositions and sizes cover all regions of observed features in these stellar objects. In addition, HD 44179 was studied by *Spitzer* and unknown mid-infrared resonances in the 13–20 μm range were observed (Markwick-Kemper, Green & Peeters 2005). A broad peak at 13–17 μm was found and a mixture of Mg–Fe oxides with unknown material was proposed as a carrier (Markwick-Kemper et al. 2005). It is possible that cement nanoparticles contribute to this peak.

Oxygen is one of the chemical elements for which depletion in the gas phase has been observed over many sightlines (Jenkins 2009; Whittet 2010; Jenkins 2014). It is known that in cosmic dust O atoms exist in silicates and metallic oxides. However, depletion of O atoms is much higher than, for example, depletion of Mg, Si or Fe and can be even greater by a factor of 16 (Jenkins 2009). Existing dust-grain composition models cannot explain this. The ratio of numbers of O atoms and Mg+Si atoms, even in the oxygen-rich $MgSiO_3$, is 1.5. The ratio O/(Ca+Si) in our clusters C1, C2 and C3 is 1.75, 1.44 and 3.25, respectively. Therefore, the number of oxygen atoms in cementitious nanoparticles is large and could help in the explanation of its depletion in the interstellar medium. A similar conclusion for the nanopyroxene cluster $Mg_4Si_4O_{12}$ has been reached by Goumans and Bromley (Goumans & Bromley 2011).

4 CONCLUSIONS

Silicates are one of the main components of cosmic dust grains. However, their precise chemical composition is not known. To the pool of possible silicate materials in cosmic dust we have added cement. We have studied one crystalline and two amorphous Ca–Si–H–O clusters, which represent the chemical composition and

Table 2. Silicate infrared bands at (9.7–11) and 18 μm, as well as specific cement bands around 14 μm, for nanoparticles C1 (crystalline precursor), C2 (amorphous) and C3 (amorphous). Silicate and unidentified bands in the same spectral intervals of three stellar objects (Molster et al. 2002a) are also shown. Uncertain detections in the spectra of cosmic objects are marked by '?'.

Object	Bands (μm)
C1	10.26, 10.29, 10.40, 10.47, 10.63, 11.02, 11.11, 11.34, 11.59, 11.61, 11.62, 11.75, 14.44, 14.55
C2	9.91, 10.18, 11.46, 11.73, 13.71, 14.10, 14.32, 18.38
C3	9.74, 9.81, 10.27, 10.40, 11.05, 11.28, 11.60, 11.61, 13.63, 13.79, 14.58, 14.94, 18.02, 18.29, 18.58, 18.99
HD 45677	9.81, 9.99, 10.57, 11.06, 11.50, 13.54, 13.77, 14.3, 18.06, 18.88
HD 44179	10.8?, 13.58, 14.19, 18.03, 18.97
IRC+10420	10.6, 10.7?, 11.04, 13.51, 13.76, 14.15, 18.2

Table 3. Bands observed for stellar objects above 19 μm (Molster et al. 2002a) and the corresponding bands of cement nanoparticles. Only bands with intensities above 10 km mol^{-1} are shown for C1, above 15 km mol^{-1} for C2 and above 50 km mol^{-1} for C3. We expect that dust close to some oxygen-rich stars consists of other silicates and oxides, as well as of a mixture of cement nanoparticles of various sizes, compositions and infrared band positions.

Object	Bands (μm)
HD 45677	19.43, 20.67, 21.59, 22.41, 22.95, 23.67, 24.52, 25.04, 26.07, 26.93, 27.75, 28.30, 29.37, 30.61, 32.33, 32.79, 33.65, 34.5, 35.6, 38.21, 39.87, 40.64, 41.70, 42.95, 43.60, 44.90
HD 44179	19.65, 20.77, 21.59, 22.86, 23.81, 24.65, 24.99, 26.08, 27.69, 28.26, 29.44, 30.77, 32.51, 33.03, 33.70, 34.35, 35.28, 36.02, 36.53, 40.46, 43.5, 48.0, 56.6, 65.6, 69.02
IRC+10420	20.70, 21.45, 22.96, 23.73, 24.16, 26.01, 27.48, 27.97, 32.56, 32.99, 33.54, 34.82, 35.95, 40.37, 41.5, 43.00, 44.39, 47.83, 49.07, 54.9, 61.6
C1	19.08, 21.22, 21.73, 21.96, 22.96, 23.11, 24.76, 26.25, 27.51, 28.16, 29.22, 31.22, 33.01, 33.60, 35.92, 36.44, 36.86, 38.76, 39.40, 46.31, 47.68, 48.39, 50.48, 50.89, 58.74, 60.51, 69.06
C2	20.60, 20.92, 21.53, 21.64, 22.53, 22.90, 23.69, 24.03, 24.82, 25.49, 26.59, 29.42, 29.90, 32.16, 32.52, 33.05, 34.47, 37.08, 37.93, 39.55, 41.24, 43.43, 52.32, 57.04, 58.58
C3	19.84, 20.68, 21.47, 21.50, 22.40, 22.86, 23.76, 24.18, 24.30, 24.59, 24.88, 25.96, 26.43, 26.69, 27.68, 27.84, 28.98, 29.42, 30.95, 31.34, 32.14, 32.65, 33.35, 39.69, 41.09, 64.93

bonding of cement at the nanoscale. Their infrared spectra are calculated and it is found that bands are distributed over the entire infrared spectrum. We propose that the features at 14 μm, measured by the *Infrared Space Observatory* in the dust shells of several oxygen-rich stars and currently classified as unidentified (Molster et al. 2002a,b), are cement bands. From the abundance of Ca and other chemical elements, we do not expect that cement nanoparticles are dominant species in cosmic dust. However, cementitious nanoparticles, because of the many oxygen atoms they consist of, could act as an additional reservoir of O in cosmic dust and help in the solution of its depletion in the interstellar medium. With a recent detection of Ca-rich supernovae that produce much larger amounts of calcium then previously expected (Perets et al. 2010; Kawabata et al. 2010), as well as discoveries of water everywhere in space by the *Spitzer* and *Herschel* missions (van Dishoeck, Herbst & Neufeld 2013), all the necessary ingredients for the formation of cement nanoparticles in space are readily available.

ACKNOWLEDGEMENTS

This work has been carried out using the computer cluster 'Isabella' at the University of Zagreb Computing Centre SRCE. GB acknowledges the support of the University of Zagreb research fund, grant 'Physics of Stars and Cosmic Dust'. We are grateful to Goran Baranović for useful discussions. We thank the editor, Keith Smith, and the anonymous referee for their constructive comments and suggestions, which have greatly improved the clarity of this manuscript.

REFERENCES

Allen A. J., Thomas J. J., Jennings H. M., 2007, Nature Materials, 6, 311
Bahn S., Jacobsen K. W., 2002, Comput. Sci. Eng., 4, 56
Bauschlicher C. W. et al., 2010, ApJS, 189, 341
Bensted J., 1976, J. Am. Ceram. Soc., 59, 140
Bhat P. A., Debnath N. C., 2011, J. Phys. Chem. Sol., 72, 920
Bilalbegovic G., 2003, Phys. Lett. A, 308, 61
Boersma C. et al., 2014, ApJS, 211, 8
Ciesla L. et al., 2014, A&A, 565, A128
Delgado A. H., Paroli R. M., Beaudoin J. J., 1996, Appl. Spectrosc., 50, 970
Draine B. T., 2011, Physics of the Interstellar and Intergalactic Medium. Princeton Univ. Press, Princeton, NJ
Enkovaara J. et al., 2010, J. Phys.: Condens. Matter, 22, 253202
Frederiksen T., Paulsson M., Brandbyge M., Jauho A. P., 2007, Phys. Rev. B, 75, 205413
Garbev K., Stemmermann P., Black L., Breen C., Yarwood J., Gasharova B., 2007, J. Am. Ceram. Soc., 90, 900
Gibb E. L., Whittet D. C. B., Boogert A. C. A., Tielens A. G. G. M., 2004, ApJS, 151, 35
Goumans T. P. M., Bromley S. T., 2011, MNRAS, 414, 1285
Grossman L., Larimer J. W., 1974, Rev. Geophys., 12, 71
Hartmann J., 1904, ApJ, 19, 268
Henning T., 2010, ARA&A, 48, 21
Hofmeister A. M., Bowey J. E., 2006, MNRAS, 367, 577
Hulkko E., Lopez-Acevedo O., Koivisto J., Levi-Kalisman Y., Kornberg R. D., Pettersson M., Hakkinen H., 2011, J. Am. Chem. Soc., 133, 3752
Jager C., Posch T., Mutschke H., Zeidler S., Tamanai A., de Vries B. L., 2011, in Cernicharo J., Bachiller R., eds, Proceedings of the International

Astronomical Union Vol. 280, 'The Molecular Universe', Cambridge Univ. Press, Cambridge, p. 416
Jain A. et al., 2013, APL Materials, 1, 011002
Jenkins E. B., 2009, ApJ, 700, 1299
Jenkins E. B., 2014, ArXiv e-print: 1402.4765
Jiang D., Walter M., 2011, Phys. Rev. B, 84, 193402
Kawabata K. S. et al., 2010, Nat, 465, 326
Kessler-Silacci J. et al., 2006, ApJ, 639, 275
Kimura Y., Nuth J. A., 2005, ApJ, 630, 637
Koike C. et al., 2001, A&A, 363, 1115
Li A., Draine B. T., 2001, ApJ, 550, L213
Manzano H., Ayuela A., Dolado J. S., 2007, J. Computer-Aided Materials Design, 14, 45
Markwick-Kemper F., Green J. D., Peeters E., 2005, ApJ, 628, L119
Martin R. M., 2004, Electronic Structure. Cambridge University Press, Cambridge
Masoero E., Gado E. D., Pellenq R. J. M., Ulm F. J., Yip S., 2012, Phys. Rev. Lett., 109, 155503
Molster F. J., Waters L. B. F. M., Tielens A. G. G. M., Barlow M. J., 2002a, A&A, 382, 184
Molster F. J., Waters L. B. F. M., Tielens A. G. G. M., 2002b, A&A, 382, 222
Mortensen J. J., Hansen L. B., Jacobsen K. W., 2005, Phys. Rev. B, 71, 035109
Mutschke H., Zeidler S., Posch T., Kerschbaum F., Baier A., Henning T., 2008, A&A, 492, 117
Nobst P., Stark J., 2003, Cem. Concr. Compos., 25, 899
Pellenq R. J. M., Kushima A., Shahsavari R., van Vliet K. J., Buehler M. J., Yip S., Ulm F. J., 2009, Proc. Nat. Acad. Sci. USA, 106, 16102
Perdew J. P., Burke K., Ernzerhof M., 1996, Phys. Rev. Lett., 77, 3865
Perets H. B. et al., 2010, Nat, 465, 322
Porezag D., Pederson M. R., 1996, Phys. Rev. B, 54, 7830
Ricca A., Bauschlicher C. W., Allamandola L. J., 2013, ApJ, 776, 31
Simon J. I., DePaolo D. J., Moynier F., 2009, ApJ, 702, 707
Skinner L. B., Chae S. R., Benmore C. J., Wenk H. R., Monteiro P. J. M., 2010, Phys. Rev. Lett., 104, 195502
Tielens A. G. G. M., 2013, Rev. Mod. Phys., 85, 1021
van Boekel R., Min M., Waters L. B. F. M., de Koter A., Dominik C., van den Ancker M. E., Bouwman J., 2005, A&A, 437, 189
van Dishoeck E. F., Herbst E., Neufeld D. A., 2013, Chem. Rev., 113, 9043
Wada S., Sakata A., Tokunaga A. T., 1991, ApJ, 375, L17
Wales D. J., Doye J. P. K., 1997, J. Phys. Chem. A, 101, 5111
Wales D. J., Scheraga H. A., 1999, Science, 285, 1368
Watson D. M. et al., 2009, ApJS, 180, 84
Whittet D. C. B., 2010, ApJ, 710, 1009
Whittet D. C. B. et al., 1997, ApJ, 490, 729
Yu P., Kirkpatrick R. J., Poe B., McMillan P. F., Cong X., 1999, J. Am. Ceram. Soc., 82, 742

This paper has been typeset from a TEX/LATEX file prepared by the author.